

孙晓旭, 冯坚, 李超, 等. 自动矿物识别和表征系统在辽东吉祥峪稀土矿矿物鉴定和赋存状态研究中的应用 [J]. 岩矿测试, 2023, 42(6): 1120–1131. doi: [10.15898/j.ykcs.202203270061](https://doi.org/10.15898/j.ykcs.202203270061).

SUN Xiaoxu, FENG Jian, LI Chao, et al. Application of Automated Mineral Identification and Characterization System to Identify Minerals and Occurrences of Elements in Jixiangyu Rare Earth Deposit of Eastern Liaoning [J]. Rock and Mineral Analysis, 2023, 42(6): 1120–1131. doi: [10.15898/j.ykcs.202203270061](https://doi.org/10.15898/j.ykcs.202203270061).

自动矿物识别和表征系统在辽东吉祥峪稀土矿矿物鉴定和赋存状态研究中的应用

孙晓旭, 冯坚, 李超, 高野, 王雷, 苗彤, 徐杨, 闫伟
(辽宁省地质矿产研究院有限责任公司, 辽宁沈阳 110032)

摘要: 辽宁省已知的稀土矿类型较少, 以往稀土矿床的勘查评价偏重于独居石砂矿和碱性岩型稀土矿, 沉积变质型稀土矿涉及较少, 其矿石学、矿物学研究程度偏低。本文以吉祥峪稀土矿床为研究对象, 应用自动矿物识别和表征系统(AMICS), 结合高分辨率扫描电子显微镜(SEM)和高通量能谱仪(EDS)对矿石进行分析, 获得吉祥峪稀土矿石中矿物化学成分、元素赋存状态及矿物共生组合关系。结果表明, 矿石中稀土元素以La、Ce、Pr、Nd等轻稀土元素为主; 主要稀土矿物为独居石(0.73%)、褐帘石(6.25%)、方铈石(0.25%)和磷灰石(类质同象)等; 通过背散射图像结合光学显微镜观察得出矿石中的褐帘石、独居石、方铈石及磷灰石等具有较好的连生关系, 这些矿物以单颗粒或聚粒结构与磁铁矿交叉镶嵌, 或分布在磁铁矿边缘及间隙中。矿石中稀土矿物与磁铁矿密切共生, 含量呈正相关, 其原因可能为: ①沉积富集。吉祥峪稀土矿位于辽吉裂谷的核部, 裂谷为矿床提供了有利的沉积环境。②岩浆改造。岩浆热液可能与里尔峪一段变粒岩产生反应, 使其中的稀土和铁元素集聚。③构造控制。吉祥峪稀土矿位于吉祥峪—算盘峪背斜核部穹隆之上, 构造发育, 断裂带和褶皱可能在地壳的应力作用下形成矿物质富集的通道, 使矿质从深部运移至浅部。

关键词: 自动矿物识别和表征系统(AMICS); 沉积变质型稀土矿; 独居石; 褐帘石; 磁铁矿; 稀土矿物赋存状态

要点:

- (1) 辽东吉祥峪稀土矿稀土矿物主要为独居石、褐帘石、方铈石和磷灰石。
- (2) 褐帘石、独居石、方铈石及磷灰石具有较好的连生关系, 这些矿物以单颗粒、聚粒结构与磁铁矿交叉镶嵌, 或分布在磁铁矿边缘和间隙中。
- (3) 矿石中磁铁矿与稀土矿物含量及分布呈正相关, 其原因可能主要为矿质的原始沉积富集, 其次可能受到岩浆、构造活动的控制、叠加改造。

中图分类号: P575 **文献标识码:** A

中国稀土资源丰富、种类齐全, 稀土资源量占全球稀土资源总量的近一半。中国目前已发现的矿床类型有碱性岩型、花岗岩型、碳酸盐型和沉积变质型等类型, 已发现的稀土矿物有30余种, 如氟碳铈矿、

独居石、硬钽矿、磷钇矿、铈钆钇矿和棱锰矿等^[1]。中国内生稀土矿床多分布在长江以南地区, 大地构造位置如扬子准地台、华南褶皱系、松潘—甘孜褶皱系、东南沿海褶皱系等, 北方地区由于华北克拉通相

收稿日期: 2022-03-27; 修回日期: 2022-05-23; 接受日期: 2023-07-24

基金项目: 辽宁省省级地质勘查项目“辽宁省辽阳县吉祥峪稀土矿预查”(JH20-210000-05760)

作者简介: 孙晓旭, 硕士, 高级工程师, 主要从事区域地质调查和矿产勘查工作。E-mail: 656546966@qq.com。

对稳定, 缺乏形成富集稀土元素的构造环境, 仅在中朝准地台边缘出现一些稀土矿床, 如内蒙古白云鄂博、山东微山郗山、辽宁凤城赛马、辽宁辽阳生铁岭等矿床^[2-3]。

辽宁省已知稀土矿类型稀少, 且以往稀土矿床的勘查评价多偏重于独居石砂矿和碱性岩型稀土矿, 沉积变型稀土原生矿涉及较少, 矿石学、矿物学研究程度偏低。辽宁省在开展稀土矿产潜力评价工作时曾对省内的沉积变型矿床(生铁岭稀土矿)成矿模式进行研究, 总结了其成矿地质环境及矿床特征, 认为其为含有少量独居石的磷灰岩型矿床^[4]。籍魁^[5]对辽宁辽阳郭家稀土矿床地质特征进行了研究, 发现其矿石矿物主要为独居石、褐帘石, 矿床类型为与古火山构造有关的沉积变质再造型矿床。本文研究的吉祥峪稀土矿床与生铁岭、郭家稀土矿床类型相似, 矿石中稀土含量可观, 但稀土矿物赋存状态、稀土元素在矿物中的分布规律以及稀土矿物能否被提取利用等问题尚需得到解决^[6-7]。

自动矿物识别和表征系统(AMICS)是以成分点原位分析为基础, 连接高分辨率扫描电镜(SEM)和高通量能谱仪(EDS), 采用矿物边界分区法及图形处理技术, 结合频谱列表快速、全面地对光谱进行合并及分类, 比照矿物数据库自动拟合计算, 能高效、全面、精确地测定样品的矿物成分、元素分布、粒度、连生关系以及孔隙度等信息, 在含量低、颗粒细小的矿物定性、定量测试方面是一套先进、可行的技术方法^[8-12]。该方法被广泛应用于地质、冶金等领域。例如, 葛祥坤等^[13]和张然等^[14]运用该系统对鄂尔多斯盆地砂岩型铀矿物进行定量分析, 查明了铀矿物类型和其他伴生矿物; 温利刚等^[15-18]、罗晓锋等^[19]将该系统应用于稀土矿物的赋存状态研究, 查明了稀土矿物种类和含量; 王恩雷等^[20]运用该系统对海城菱镁矿进行工艺矿物学研究, 发现其矿物粒度细、脉石矿物与菱镁矿连生是矿石难选的主要原因; 胡欢等^[21]运用该系统研究了金属铍赋存状态, 认为其对低含量铍元素的准确分析和微细含铍矿物的识别有良好的效果; 范雨辰等^[22]运用该系统对页岩储集空间的微观展布样式进行表征分类, 通过扫描孔隙-矿物接触面积计算出孔隙类型和占比, 有效地表征了含油(沥青)的储集空间。

因此, 本文采用 AMICS 自动矿物识别和表征系统对正在开展勘查评价工作的吉祥峪稀土矿床进行矿物识别, 目的是获得稀土元素在矿物中的分布规律, 查明稀土矿物的种类和赋存状态, 通过分析稀土

矿物及相关矿物的成分、结构和嵌布特征, 研究其成矿机制, 揭示稀土矿床形成的约束条件, 为矿床的勘查评价和有效利用提供矿物学依据。

1 地质背景

吉祥峪稀土矿床大地构造位置处于华北陆块北缘, 辽吉古元古代裂谷核部, 吉祥峪—算盘峪背斜的核部。研究区出露地层主要为辽河群里尔峪组(Pt₁lr)、高家峪组(Pt₁g)和大石桥组(Pt₁d), 属于一套火山碎屑沉积变质建造(图 1)^[23-26]。本次发现的稀土矿体严格受里尔峪组一段浅粒岩夹变粒岩层位控制。钻孔中所取的基本分析样测试结果显示, 矿石中铁平均品位为 25.07×10^{-2} , 稀土平均品位为 1.03×10^{-2} , 轻稀土元素占绝对优势(以镧铈为主, 钐铕镨钕等次之)。矿石主要结构构造为粒柱状变晶结构, 块状及条带状构造: 磁铁矿、角闪石、黑云母、褐帘石等暗色矿物集聚组成深色条纹条带, 与长石、磷灰石等组成的浅色矿物条带相间排列。稀土矿体呈似层状、扁豆状顺层产出里尔峪组一段磁铁浅粒岩夹褐帘磷灰磁铁变粒岩层位中, 与其顶底板浅粒岩呈整合渐变关系。主要的蚀变类型有碳酸盐化、云母化、绿帘石化和碎裂岩化。

2 实验部分

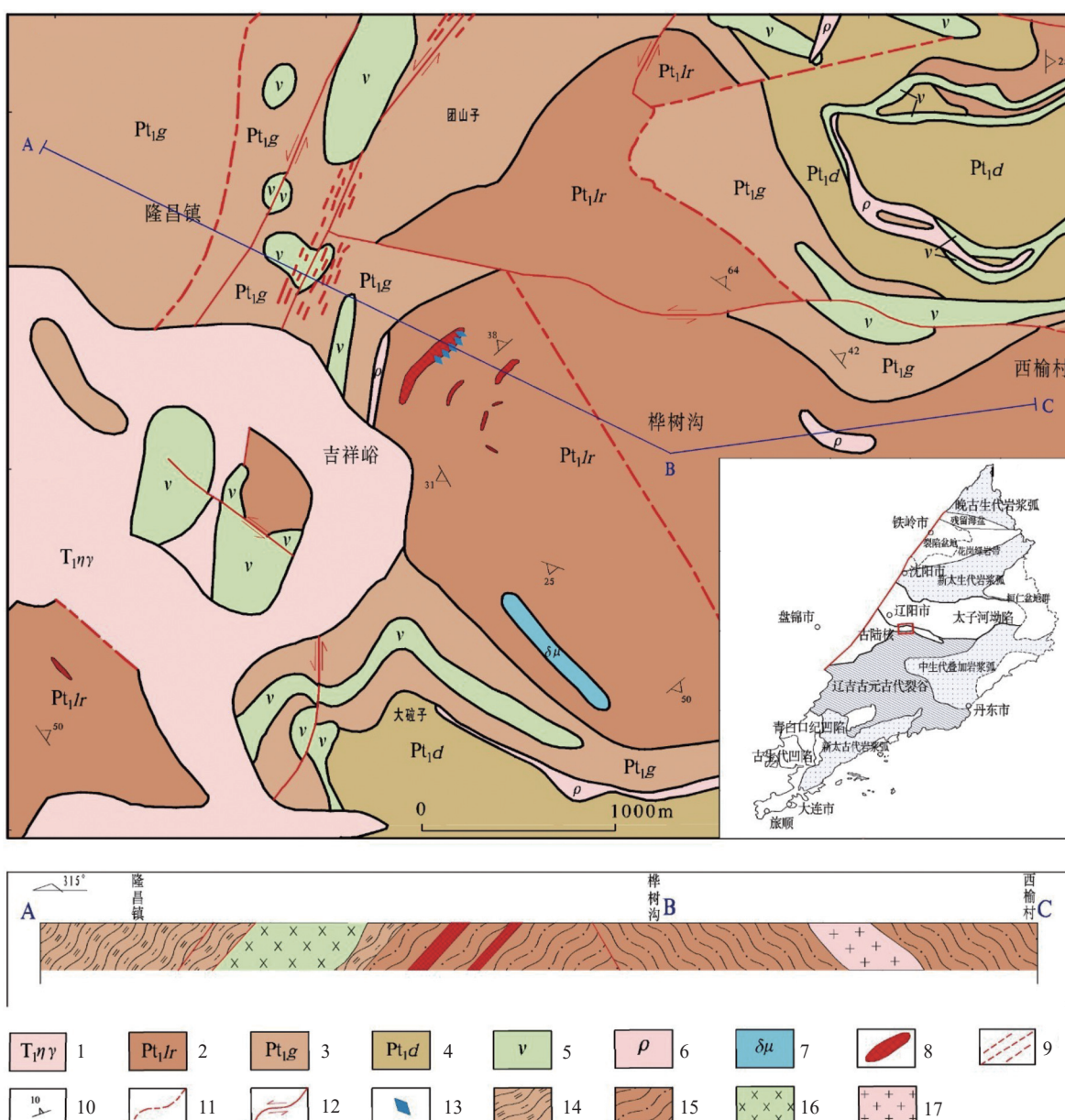
2.1 样品采集与制备

本次实验样品采集于辽阳县隆昌镇吉祥峪研究区钻孔岩心, 岩性为磷灰褐帘磁铁角闪变粒岩(样品编号 XT-02), 样品颜色为灰黑色, 鳞片粒状变晶结构, 块状构造。测试前先将样品混合破碎至 1mm 以下, 筛出 22~120 目样品置于环氧树脂中抛磨出光滑平面, 真空喷碳增加导电性, 然后进行 AMICS 分析^[27-28]。

2.2 实验仪器及测试条件

实验测试在河南省岩石矿物测试中心完成。实验仪器包括一台超高分辨率场发射扫描电镜(Zeiss Sigma 500)、一台电制冷能谱仪(Bruker XFlash6610)以及一套 AMICS 自动矿物识别和表征系统。

本次测试仪器均经过调整和标定, 并引入了质控样品用于监测和验证仪器性能和数据准确性, 对 XT-02 样品进行重复测试以检查数据的重复性和精确性, 测试过程中出现“计数率低”和“未识别”时调整测试参数和颗粒数, 以保证测试数据的可靠性。测试时实验条件为: 高真空环境, 加速电压 20kV, 工作距离 11.8mm, 点分析采集时间达到 250kcps 自动停止。



1—晚三叠纪二长花岗岩；2—里尔峪岩组；3—高家峪岩组；4—大石桥岩组；5—辉长岩；6—伟晶岩；7—闪长玢岩；8—稀土矿体；9—韧性剪切带；10—岩层产状；11—推断断裂；12—实测断裂；13—采样位置；14—二云片岩花纹；15—浅粒岩花纹；16—辉长岩花纹；17—伟晶岩花纹。

图1 吉祥峪稀土矿床地质简图及研究区位置图

Fig. 1 Geological map and location map of Jixiangyu rare earth deposit. 1—Late Triassic monzogranite; 2—Lieryu Formation; 3—Gaojiayu Formation; 4—Dashiqiao Formation; 5—Gabbro; 6—Pegmatite; 7—Diorite porphyrite; 8—Rare earth ore body; 9—Ductile shear zone; 10—Occurrence of rock formation; 11—Presumed fault; 12—Measured fault; 13—Sampling location; 14—Two-mica schist pattern; 15—Leptite pattern; 16—Gabbro pattern; 17—Pegmatite pattern.

3 结果与讨论

3.1 稀土矿物的种类

通过矿物自动分析技术完成了稀土矿物的识别，确定组成稀土矿石样品(XT-02)的矿物类型10余种，主要矿物有：磁铁矿、阳起石、褐帘石、磷灰石、独居石、方铈石，次要矿物有：石英、斜长石、钾长石、榍

石、黑云母。矿石矿物含量由高至低依次为：磁铁矿63.48%、阳起石7.61%、石英7.36%、褐帘石6.25%、磷灰石5.73%、钾长石2.20%、斜长石2.14%、独居石0.73%、黑云母0.51%、榍石0.39%、方铈石0.25%、绿泥石0.14%、钙铁榴石0.01%、锆石0.01%(图2、表1)。由此可知，吉祥峪稀土矿主要含

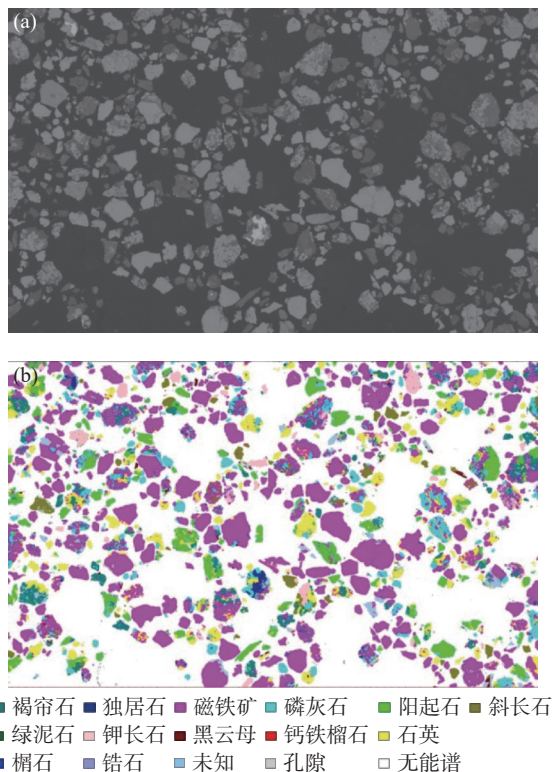


图2 吉祥峪稀土矿床样品(a)电子图像和(b)AMICS分析结果

Fig. 2 Electron image (a) and AMICS analysis result (b) of Jixiangyu rare earth deposit sample.

稀土矿物为褐帘石、独居石、方铈石和磷灰石。

3.1.1 褐帘石

褐帘石是一种含有较高稀土组分的帘石族矿物, 其轻稀土成分可占全岩类的 90% 以上, 其中 Ca 可

被 REE³⁺、Th⁴⁺、U⁴⁺等替代, 使其高度富集 LREE、U、Th 等微量元素, 化学成分变化较大, Al 可被 Fe²⁺、Mg²⁺等替代^[31-32]。

褐帘石在 XT-02 样品中分布不均匀, 含量为 6.25%。样品中的褐帘石多呈柱状或厚板状, 解理不完全, 自形-半自形, 粒径 0.01~0.595mm。对其进行能谱分析, 得到褐帘石平均含有 O 37.07%、Fe 16.38%、Si 11.88%、Ca 7.96%、Al 5.35%、Mg 0.55%、Ce 10.69%、La 6.79%、Nd 2.24%、Pr 1.09%(表 2)。矿物中富含轻稀土元素, 以 Ce、La、Nd 为主, 含少量 Pr, 未见 U 元素和 Th 元素的替代^[33-34]。镜下观察发现, 褐帘石常与磷灰石、磁铁矿连生, 与磁铁矿关系密切(图 3a; 图 4 中 a, c)。

3.1.2 方铈石

方铈石在 XT-02 样品中少量分布, 多以单体形式存在, 含量为 0.25%。样品中方铈石常呈不规则粒状及聚粒状, 粒径 0.01~0.5mm(图 3b)。对其进行能谱分析, 得到方铈石平均含有 Ce 53.67%、O 21.07%、Fe 8.56%、Si 3.67%、P 3.36%、Pr 2.35%、Nd 1.79%、Ca 1.30%、Th 1.29%、Al 1.23%、La 0.87%、Mn 0.56%、Mg 0.28%(表 3), 矿物中富含轻稀土元素, 以 Ce、La、Nd 为主, 常见 Mg 元素等被 Th 元素替代^[35]。

3.1.3 独居石

独居石是一种富含轻稀土元素的磷酸盐矿物, 含有放射性元素 Th、U。独居石常与绿泥石、阳起石等变质矿物交叉共生或作为包裹体镶嵌其中

表1 吉祥峪稀土矿床样品 AMICS 矿物定量分析结果

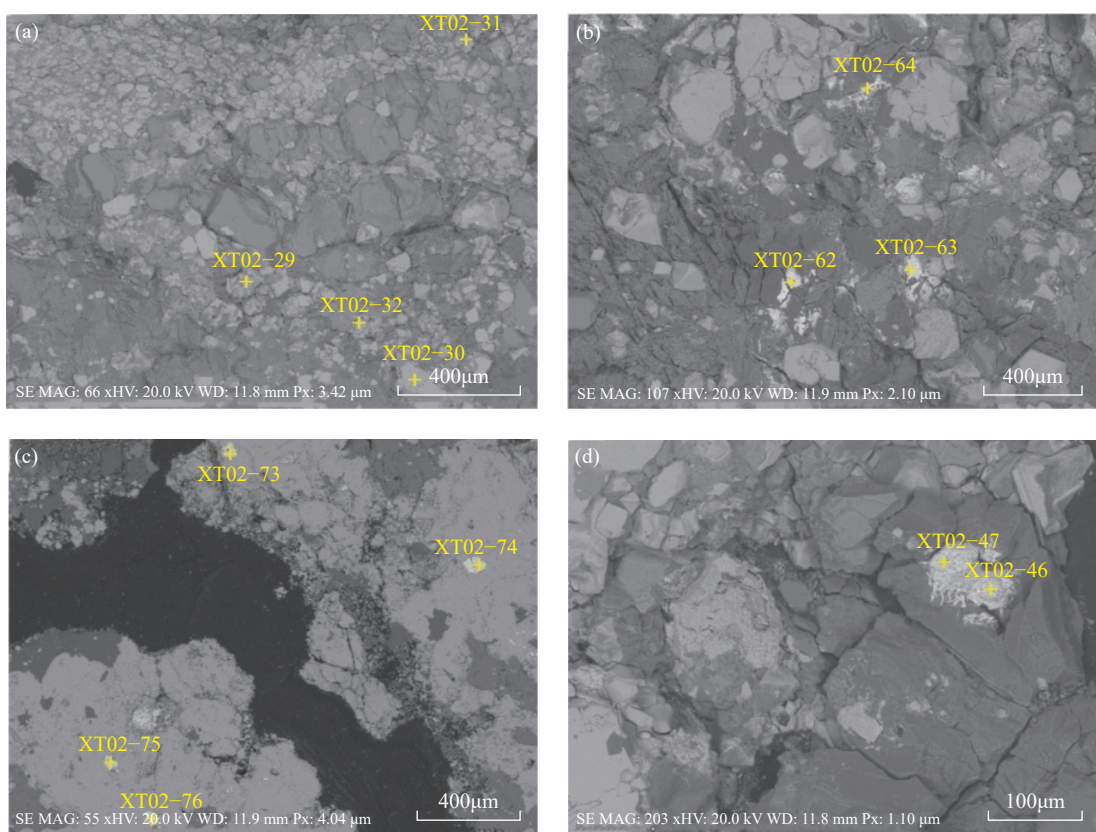
Table 1 Quantitative analysis results of minerals measured by AMICS in Jixiangyu rare earth deposit.

矿物名称	质量分数 (%)	面积百分比 (%)	统计面积 (μm ²)	颗粒数 (个)	统计相对误差 (%)	矿物标准分子式 ^[29-30]
褐帘石	6.25	6.62	3386157.37	809	0.14	(Ce, Ca)(Ce, La)(Nd, Pr)(Fe ²⁺ , Fe ³⁺)(Al, Mg)[Si ₂ O ₇][SiO ₄]O(OH)
独居石	0.73	0.57	289757.48	105	0.35	(Ce, La, Ca, Fe, Th, Nd, Pr)[SiO ₄] [PO ₄]
方铈石	0.25	0.50	257590.30	78	0.06	(Ce ³⁺ , Th, Fe, Pr, Nd)O ₂
磷灰石	5.73	7.22	3696466.51	861	0.10	Ca ₅ [PO ₄] ₃ (F, OH)
磁铁矿	63.48	48.95	25056614.78	1891	0.07	Ca ₂ Na(Mg, Fe) ₅ (Al, Fe ³⁺) ₂ [(Si, Al) ₄ O ₁₁] ₂ (OH) ₂
阳起石	7.61	9.94	5088796.43	524	0.11	SiO ₂
石英	7.36	11.16	5713847.71	1218	0.08	Ca ₃ Fe ₂ [SiO ₄] ₃
钙铁榴石	0.01	0.01	70.14	1	2.00	Na[AlSi ₃ O ₈]
斜长石	2.14	3.25	1663198.10	288	0.16	CaTi[SiO ₄]O
榍石	0.39	0.44	227134.51	301	0.20	Zr(SiO ₄)
绿泥石	0.14	0.19	99300.33	166	0.18	Fe ²⁺ [Si ₄ O ₁₀](OH) ₂ (Mg, Al, Fe, Si) ₃ (OH) ₆
钾长石	2.20	3.41	1743721.36	134	0.21	K[AlSi ₃ O ₈]
黑云母	0.51	0.65	334115.41	344	0.15	K(Fe, Al) ₃ AlSi ₃ O ₁₀ (F, OH) ₂
未知矿物	3.20	6.36	3255145.74	4728	0.05	/
孔隙	/	0.73	371809.84	22084	0.06	/

表2 褐帘石能谱分析结果

Table 2 Energy spectrum analysis results of allanite.

样品编号	质量分数(%)									
	O	Fe	Si	Ca	Al	Mg	Ce	La	Nd	Pr
XT02-07	37.43	16.07	11.74	7.76	5.27	0.59	11.06	6.95	2.04	1.08
XT02-13	35.73	15.11	12.31	7.76	5.50	0.59	11.60	7.81	2.33	1.25
XT02-29	38.23	15.73	11.30	8.39	5.02	0.41	10.94	7.07	1.94	0.98
XT02-30	37.13	17.78	11.63	8.06	5.17	0.47	10.27	6.18	2.31	1.00
XT02-31	36.85	16.50	12.80	7.41	6.17	0.82	9.77	6.17	2.26	1.25
XT02-32	37.03	17.08	11.49	8.39	4.99	0.42	10.48	6.58	2.54	1.00
平均值	37.07	16.38	11.88	7.96	5.35	0.55	10.69	6.79	2.24	1.09



a—褐帘石; b—方铈石; c—粒状独居石; d—放射状独居石。

图3 稀土矿物背散射图像

Fig. 3 Backscattering images of rare earth ores: (a) Allanite; (b) Cerianite; (c) Granular monazite; (d) Radial monazite.

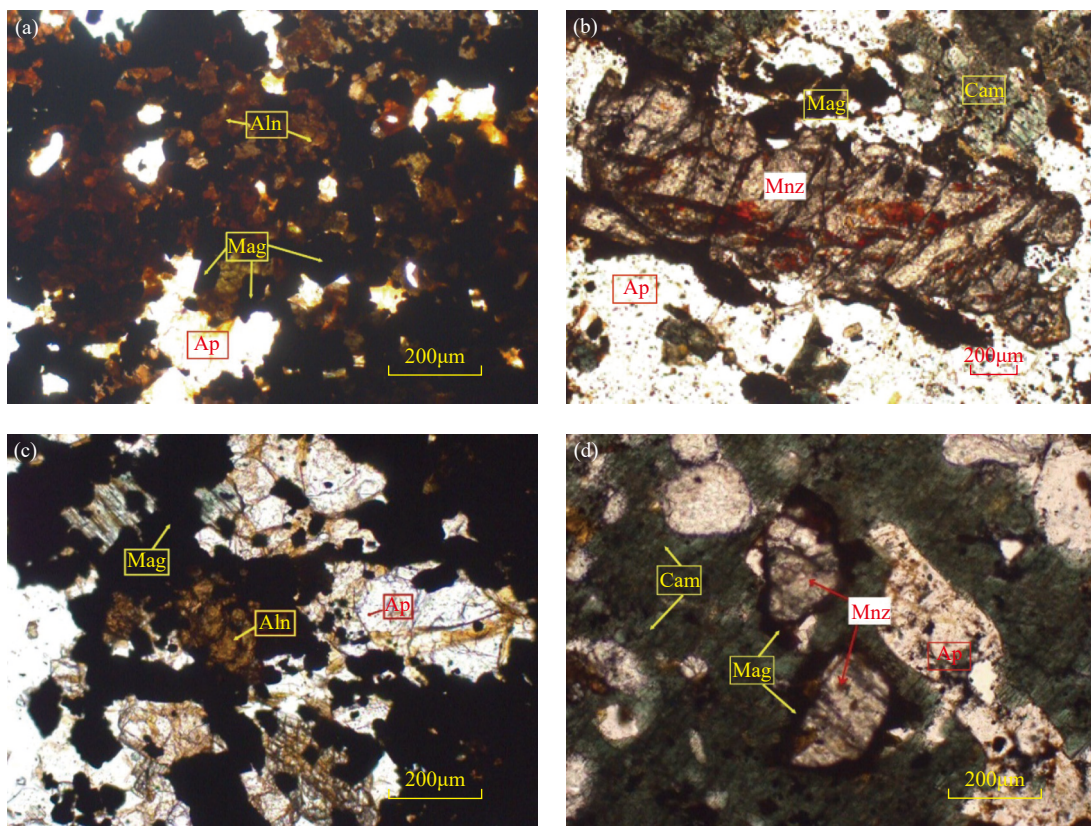
(图3中c,d)。在背散射图像中,独居石较其他矿物具有更高的亮度,其亮度与Th含量呈正比^[36-38]。

独居石在XT-02样品中多以单体形式存在,含量为0.73%。样品中的独居石呈自形-半自形板状,解理完全,粒径0.01~2.1mm。对其进行能谱分析,得到独居石平均含有O 29.38%、P 13.87%、Ce 20.08%、La 20.43%、Nd 8.68%、Pr 2.92%、Ca 1.55%、Fe 1.05%、Si 0.81%、Th 1.25%(表4)。矿物中富含轻

稀土元素,以Ce、La、Nd为主,常见Ca元素等被Th元素替代。镜下观察发现,独居石与磁铁矿连生,常被褐帘石、磷灰石等矿物包裹^[39](图4中b,d)。

3.1.4 其他含稀土矿物

矿石中还含有磷灰石(5.73%)。磷灰石是一种重要的稀土元素累积矿物,其在变质岩中作为常见的副矿物出现,已报道的磷灰石中的稀土含量最高可达11.14%(RE_2O_3),且主要为轻稀土^[40-41]。饶金



a—褐帘石与磷灰石、磁铁矿连生; b—独居石被磷灰石包裹; c—褐帘石与磷灰石连生, 被磁铁矿包裹; d—独居石与磁铁矿连生, 被角闪石包裹。Aln—褐帘石; Ap—磷灰石; Mag—磁铁矿; Mnz—独居石; Cam—角闪石。

图4 样品XT-02(磷灰褐帘磁铁角闪变粒岩)的显微组构特征

Fig. 4 Microfabric characteristics of sample XT-02 (apatite-allanite-magnet-hornblende granulite): (a) Allanite, apatite and magnetite coexisting; (b) Monazite surrounded by apatite; (c) Allanite and apatite coexisting, surrounded by magnetite; (d) Monazite associated with magnetite and wrapped by amphibole. Aln—Allanite; Ap—Apatite; Mag—Magnetite; Mnz—Monazite; Cam—Amphibole.

表3 方铈石能谱分析结果

Table 3 Energy spectrum analysis results of cerianite.

样品编号	质量分数(%)												
	Ce	O	Fe	Si	P	Pr	Nd	Ca	Th	Al	La	Mn	Mg
XT02-38	57.32	17.24	8.32	3.63	3.96	3.84	2.80	1.36	/	1.53	/	/	/
XT02-39	52.73	16.46	8.53	4.17	3.58	4.15	2.35	1.29	/	1.75	/	3.95	1.04
XT02-54	45.70	23.43	13.12	4.25	2.71	0.98	1.13	1.79	1.95	2.04	2.02	/	0.89
XT02-61	53.13	25.81	5.44	4.38	3.06	1.30	1.36	1.04	2.02	1.11	1.35	/	/
XT02-62	66.35	15.50	4.47	2.79	3.22	1.65	1.59	1.02	1.61	/	1.80	/	/
XT02-63	55.86	21.51	6.37	2.63	4.07	2.56	1.83	1.57	2.84	0.74	/	/	/
XT02-64	44.60	27.54	13.65	3.86	2.93	1.94	1.48	1.02	0.62	1.46	0.89	/	/
平均值	53.67	21.07	8.56	3.67	3.36	2.35	1.79	1.30	1.29	1.23	0.87	0.56	0.28

山等^[42]通过实验揭示了磷灰石含稀土的机制:①磷灰石包裹微细独立稀土矿物(独居石、褐帘石)(图4b)。②RE³⁺晶格替代磷灰石中的Ca²⁺。

3.2 AMICS方法的优势与不足

AMICS系统的优势明显:①以往的稀土矿物鉴定工作需要先在目镜下区分矿物,圈定矿物位置,然

表4 独居石能谱分析结果

Table 4 Energy spectrum analysis results of monazite.

样品编号	质量分数(%)									
	O	Ce	La	P	Nd	Pr	Ca	Fe	Si	Th
XT02-06	27.53	24.44	17.99	14.39	7.11	2.49	2.20	2.20	0.93	0.72
XT-02-40	21.03	12.05	28.06	14.69	12.33	4.81	3.46	2.34	0.88	0.33
XT02-46	25.81	11.32	26.81	12.77	11.69	4.49	2.40	1.35	1.71	1.65
XT02-47	26.91	9.71	26.13	13.38	11.81	4.71	2.16	1.64	1.38	2.17
XT02-53	32.08	9.84	24.95	12.25	10.93	4.13	1.90	0.89	1.07	1.96
XT02-55	31.13	20.20	19.32	13.69	7.65	2.45	4.33	1.24	/	/
XT02-56	38.95	14.45	19.58	12.79	8.18	2.67	2.06	/	1.32	/
XT02-68	39.31	14.25	18.25	11.32	6.91	2.53	3.14	2.85	0.54	0.90
XT02-69	30.77	26.29	16.70	15.64	7.28	2.30	/	/	/	1.02
XT02-71	27.88	27.67	17.08	13.91	7.96	2.16	/	0.27	0.65	2.43
XT02-73	28.40	28.23	18.51	14.91	6.78	1.99	/	0.30	/	0.88
XT02-74	26.63	27.20	17.16	14.08	7.92	2.07	/	0.39	1.01	3.55
XT02-75	28.00	27.00	17.16	14.73	7.52	2.08	/	0.82	0.77	1.91
XT02-76	26.93	28.47	18.32	15.59	7.42	2.06	/	0.38	1.01	/
平均值	29.38	20.08	20.43	13.87	8.68	2.92	1.55	1.05	0.81	1.25

后才能进行实验,且目标稀土矿物颗粒细小,光性特征复杂不易区分,这些都使得实验效率和准确性明显降低。该系统通过多种信号联合分析快速、准确地获得矿物微区准确的结构信息和化学成分。通过分析和比对大量的矿物样本图像和特征,快速、准确地识别出不同矿物类型,确定矿石的成分和矿物组合、尺寸分布、颗粒形状、矿物之间的关系等。②该系统可以对大量的样本数据进行分析和处理。能有效地识别出矿物的特征模式和相关性、潜在的规律和趋势,以指导矿产资源的合理开发利用^[43-44]。

但该方法仍然存在一些缺点:①在样品制备阶段需保证光片表面的平整度、凹凸表面及倒角会影响X射线的产生和激发。②AMICS测量的面积只有15mm²左右,选择样品时需注意所选样品的代表性。③测试过程中需尝试调整仪器参数和矿物测试颗粒数,控制测试相对误差率在10%左右,保证置信度大于95%。④分析系统不能区分同质多象及成分相似的矿物,需要人工识别分析数据,辅以岩矿鉴定知识加以辨认,改变分类结果,或者借助电子探针(EPMA)进一步确定矿物^[45-46]。

4 结论

通过AMICS测试,完成了辽东吉祥峪稀土矿石(样品编号XT-02)的原位解离分析,得到该稀土矿床稀土矿物主要为褐帘石、独居石和方铈石,其中褐帘石占矿物总量的比例为6.25%,独居石占比为

0.73%,方铈石占比为0.25%,稀土元素以La、Ce、Pr、Nd等轻稀土元素为主,且主要在褐帘石、独居石和方铈石中富集,少量稀土元素以类质同象形式赋存在磷灰石中。脉石矿物有阳起石、石英、斜长石、钾长石、榍石、黑云母等。

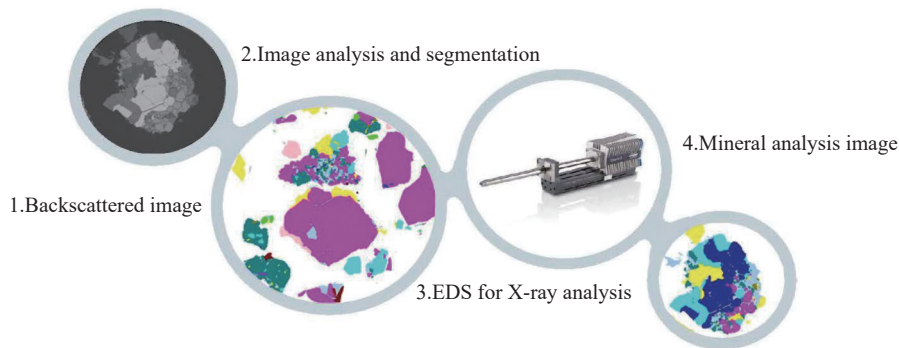
通过背散射图像结合光学显微镜观察得出,矿石中的稀土矿物褐帘石、独居石、方铈石及磷灰石具有较好的连生关系。这些矿物以单颗粒或聚粒结构与磁铁矿交叉镶嵌,或分布在磁铁矿边缘及间隙中,与磁铁矿呈现出较复杂的共生关系。该结果和样品中稀土与磁铁矿含量呈正相关相一致,分析其形成过程可能为以下原因:①沉积富集:吉祥峪稀土矿位于辽吉裂谷的核部,裂谷为矿床提供了有利的沉积环境,沉积物经过长时间的聚集、压实和蚀变作用,可能会同时释放稀土元素和铁元素并逐渐富集形成矿床。②岩浆改造:岩浆热液可能与里尔峪组一段变粒岩产生反应,形成稀土矿物和磁铁矿的矿化过程可能同时发生或相互交织,使其中高背景值的稀土元素和铁元素活化并在同一地质环境下富集。③构造控制:特定的地质过程或成矿作用可能对稀土元素和铁元素的分布产生共同的控制作用。吉祥峪稀土矿体位于辽吉裂谷带核部—吉祥峪算盘峪背斜核部的穹隆构造上,断裂带和褶皱可能在地壳的应力作用下形成矿质富集的通道,使矿质从深部运移至浅部。

Application of Automated Mineral Identification and Characterization System to Identify Minerals and Occurrences of Elements in Jixiangyu Rare Earth Deposit of Eastern Liaoning

SUN Xiaoxu, FENG Jian, LI Chao, GAO Ye, WANG Lei, MIAO Tong, XU Yang, YAN Wei
 (Liaoning Geology and Mineral Research Institute Co., Ltd., Shenyang 110032, China)

HIGHLIGHTS

- (1) The rare earth minerals in Jixiangyu rare earth deposit in Liaodong are mainly monazite, allanite, cerianite and apatite.
- (2) Allanite, monazite, cerianite and apatite have a good contiguous relationship, and these minerals are cross-inlaid with magnetite in the form of single grain or aggregate structure, or distributed in the edge and gap of magnetite.
- (3) The content and distribution of magnetite and rare earth minerals in ore deposits may exhibit a positive correlation. This relationship is primarily attributed to the original sedimentary enrichment of minerals, and secondarily, it could be influenced by magmatic and tectonic activities, as well as superimposed modifications.



ABSTRACT

BACKGROUND: In Liaoning Province, there are limited known types of rare earth deposits, and historically, exploration and evaluation efforts have mainly focused on monazite placer and alkaline rock type rare earth deposits. Less attention has been given to sedimentary metamorphic rare earth primary deposits. Previous studies have shown that the Jixiangyu rare earth deposit is categorized as a sedimentary metamorphic remodeling deposit related to ancient volcanic structures. The analysis of existing data and previous exploration results prove that this type of rare earth deposit has a considerable rare earth content with monazite and allanite. However, unresolved issues remain, such as the occurrence status of rare earth minerals and the feasibility of extracting and utilizing rare earth minerals.

OBJECTIVES: To explore the metallogenetic mechanism and unveil the formation process of rare earth deposits by identifying the types of rare earth minerals, investigating the occurrence and distribution of rare earth elements within minerals, and analyzing the composition, structure, and distribution characteristics of rare earth minerals and associated minerals.

METHODS: The experimental testing was conducted at the Henan Provincial Rock and Mineral Testing Center. The experimental instruments used in this study included an ultra-high resolution field emission scanning electron

microscope (Zeiss Sigma500), an electric cooling energy spectrometer (Bruker XFlash6610), and a set of AMICS automatic mineral identification and characterization systems. During the experiments, a high vacuum environment was maintained, with an accelerating voltage of 20kV and a beam current of 5nA. The working distance was set at 11.8mm, and the point analysis acquisition time reached 250kcps before stopping automatically.

RESULTS: The primary rare earth minerals in the Jixiangyu rare earth deposit were identified as allanite, monazite, and cerianite, constituting 6.25%, 0.73%, and 0.25% of the total mineral content, respectively. Light rare earth elements such as La, Ce, Pr, and Nd were predominantly present, enriched in monazite, xenotime, and bastnaesite, with a minor occurrence of rare earth elements in the form of solid solutions within apatite. Gangue minerals include actinolite, quartz, plagioclase, potassium feldspar, sphene, and biotite.

The rare earth minerals, including allanite, monazite, cerianite, and apatite exhibited interlocking structures with magnetite, occurring as single particles or clustered structures, and were distributed along the edges and gaps of magnetite, forming complex symbiotic relationships.

CONCLUSIONS: The rare earth formation process can be attributed to the following factors: (1) Sedimentary enrichment: The Jixiangyu rare earth deposit is situated in the core area of the Liao Ji Rift, providing favorable sedimentary conditions for ore deposition. Over time, sediments accumulated, compacted, and underwent alteration, gradually releasing and enriching rare earth and iron elements, leading to formation of the ore deposit. (2) Magmatic modification: Magmatic hydrothermal fluids may have interacted with variolitic rocks from the Lieryu section, facilitating the simultaneous or interweaving mineralization of rare earth minerals and magnetite in the same geological environment, resulting in the activation and *in situ* enrichment of high background values of rare earth and iron elements. (3) Tectonic control: The Jixiangyu rare earth deposit is situated on the anticlinal structure of the Liaoning—Jilin Paleoproterozoic rift core where fault zones and folds may have acted as channels for mineral enrichment, facilitating the migration of minerals from deeper to shallower crustal regions.

KEY WORDS: automated mineral identification and characterization system (AMICS); sedimentary metamorphic rare earth ore; monazite; allanite; magnetite; occurrence state of rare earth minerals

参考文献

- [1] 张臻悦, 何正艳, 徐志高, 等. 中国稀土矿稀土配分特征[J]. 稀土, 2016, 37(1): 121–127.
Zhang Z Y, He Z Y, Xu Z G, et al. Distribution characteristics of rare earth elements in rare earth ores in China[J]. Chinese Rare Earths, 2016, 37(1): 121–127.
- [2] 袁忠信, 白鸽. 中国内生稀有稀土矿床的时空分布[J]. 矿床地质, 2001, 20(4): 347–354.
Yuan Z X, Bai G. Temporal and spatial distribution of endogenous rare and rare earth mineral deposits in China[J]. Mineral Deposits, 2001, 20(4): 347–354.
- [3] 李童斐, 夏庆霖, 汪新庆, 等. 中国稀土矿资源成矿地质特征与资源潜力分析[J]. 地学前缘, 2018, 25(3): 95–106.
Li T F, Xia Q L, Wang X Q, et al. Geological characteristics and resource potential analysis of rare earth mineral resources in China[J]. Earth Science Frontiers, 2018, 25(3): 95–106.
- [4] 孙鹏慧. 辽宁省矿产资源潜力评价成果报告: 第一册至第六册及其工作报告[R]. 辽宁省地质矿产调查院, 辽宁省地质勘查院, 东北煤田地质局勘查设计研究院. 2013, 62–66.
Sun P H. Evaluation report on mineral resource potential in Liaoning Province, Volumes 1-6, and its work report[R]. Liaoning Geological Survey Institute, Liaoning Institute of Geological Exploration, Northeast Coalfield Geological Bureau Survey Design and Research Institute. 2013, 62–66.
- [5] 籍魁. 辽阳县郭家含稀土铁矿床矿床地质特征及成因探讨[J]. 吉林地质, 2012, 31(2): 50–54.
Ji K. Geological characteristics and genesis of the Guojia rare earth iron deposit in Liaoyang County, Liaoning Province[J]. Jilin Geology, 2012, 31(2): 50–54.
- [6] 杨占峰, 朱智慧, 王振江, 等. 白云鄂博主矿霓石型稀

- 土铁矿石中稀土元素在独立矿物中的富集状况研究[J]. 中国稀土学报, 2019, 37(6): 769–776.
- Yang Z F, Zhu Z H, Wang Z J, et al. Enrichment of rare earth elements in aegirine type rare earth iron ore in Bayan Obo mine[J]. Journal of the Chinese Society of Rare Earths, 2019, 37(6): 769–776.
- [7] 罗明标, 杨枝, 郭国林, 等. 白云鄂博铁矿石中稀土的赋存状态研究[J]. 中国稀土学报, 2007(S1): 57–61.
- Luo M B, Yang Z, Guo G L, et al. Research on occurrence state of REE in Bayan Obo iron ore[J]. Journal of the Chinese Society of Rare Earths, 2007(S1): 57–61.
- [8] Redwan M, Rammlair D, Meima J A. Application of mineral liberation analysis in studying micro-sedimentological structures within sulfide mine tailings and their effect on hardpan formation[J]. *Science of the Total Environment*, 2012, 414: 480–493.
- [9] 陈倩, 宋文磊, 杨金昆, 等. 矿物自动定量分析系统的基本原理及其在岩矿研究中的应用——以捷克泰思肯公司TIMA为例[J]. 矿床地质, 2021, 40(2): 345–368.
- Chen Q, Song W L, Yang J K, et al. Principle of automated mineral quantitative analysis system and its application in petrology and mineralogy—An example from TESCAN TIMA[J]. Mineral Deposits, 2021, 40(2): 345–368.
- [10] 刘东盛, 陈圆圆. 矿物自动分析系统在碳酸岩型稀土地球化学勘查中的应用[J]. 物探与化探, 2022, 46(3): 637–644.
- Liu D S, Chen Y Y. Application of automated mineral analysis systems in geochemical exploration of carbonatite-related REE deposits[J]. Geophysical and Geochemical Exploration, 2022, 46(3): 637–644.
- [11] 邓刘敏, 葛祥坤, 范光, 等. 基于扫描电镜-能谱仪的矿物定量分析——以AMICS为例[J]. 世界核地质科学, 2023, 40(1): 98–105.
- Deng L M, Ge X K, Fan G, et al. Quantitative analysis of minerals based on scanning electron microscope-energy dispersive spectrometer: A case study of AMICS[J]. World Nuclear Geoscience, 2023, 40(1): 98–105.
- [12] Wilhelm N, Dieter R. Automated mineralogy based on micro-energy-dispersive in comparison to a mineral liberation analyzer[J]. *Geoscientific Instrumentation Methods and Data Systems*, 2017, 6(2): 429–437.
- [13] 葛祥坤, 范光, 汪波, 等. 自动矿物分析仪用于砂岩型铀矿床矿物组成的定量分析[C]//中国核科学技术进展报告(第五卷)——中国核学会2017年学术年会论文集(第2册). 北京: 中国核学会, 2017: 125–130.
- Ge X K, Fan G, Wang B, et al. Quantitative analysis of mineral composition in sandstone-type uranium deposits using an automated mineral analyzer[C]//Advances in Chinese nuclear science and technology (Volume 5)—Proceedings of the 2017 Academic Annual Conference of the Chinese Nuclear Society (Volume 2). Beijing: Chinese Nuclear Society, 2017: 125–130.
- [14] 张然, 叶丽娟, 党飞鹏, 等. 自动矿物分析技术在鄂尔多斯盆地砂岩型铀矿矿物鉴定和赋存状态研究中的应用[J]. 岩矿测试, 2021, 40(1): 61–73.
- Zhang R, Ye L J, Dang F P, et al. Application of automatic mineral analysis technology to identify minerals and occurrences of elements in sandstone-type uranium deposits in the Ordos Basin[J]. Rock and Mineral Analysis, 2021, 40(1): 61–73.
- [15] 温利刚, 曾普胜, 詹秀春, 等. 矿物表征自动定量分析系统(AMICS)技术在稀土稀有矿物鉴定中的应用[J]. 岩矿测试, 2018, 37(2): 121–129.
- Wen L G, Zeng P S, Zhan X C, et al. Application of the automated mineral identification and characterization system (AMICS) in the identification of rare earth and rare minerals[J]. Rock and Mineral Analysis, 2018, 37(2): 121–129.
- [16] 温利刚, 贾木欣, 王清, 等. 基于扫描电子显微镜的自动矿物学新技术——BPMA及其应用前景[J]. 有色金属(选矿部分), 2021(2): 12–23.
- Wen L G, Jia M X, Wang Q, et al. A new SEM-based automated mineralogy system: BPMA and its application prospects in mining industry[J]. *Nonferrous Metals (Mineral Processing Section)*, 2021(2): 12–23.
- [17] 温利刚, 曾普胜, 詹秀春, 等. 迪纳厂矿床: 一个“白云鄂博式”铁-铜-稀土矿床[J]. 地学前缘, 2018, 25(6): 308–329.
- Wen L G, Zeng P S, Zhan X C, et al. The Yinachang deposit in Central Yunnan Province, Southwest China: A “Bayan Obo-type” Fe-Cu-REE deposit[J]. Earth Science Frontiers, 2018, 25(6): 308–329.
- [18] 温利刚, 曾普胜, 詹秀春, 等. 云南禄丰鹅头厂铁铜矿床中稀土矿物的发现及意义[J]. 岩石矿物学杂志, 2019, 38(4): 477–497.
- Wen L G, Zeng P S, Zhan X C, et al. The discovery of rare earth minerals in the Etouchang Fe-Cu deposit in Lufeng, Central Yunnan Province, and its geological

- significance [J]. *Acta Petrologica et Mineralogica*, 2019, 38(4): 477–497.
- [19] 罗晓锋, 杨占峰, 王振江, 等. 白云鄂博东矿萤石型铌-稀土-铁矿石中铌的赋存状态及分布规律 [J]. *矿物学报*, 2022, 42(5): 659–668.
- Luo X F, Yang Z F, Wang Z J, et al. Occurrence and distribution patterns of niobium in fluorite-type niobium-rare earth-iron ores from Baiyun Ebo east mine [J]. *Acta Mineralogica Sinica*, 2022, 42(5): 659–668.
- [20] 王恩雷, 李晓安, 姜效军, 等. 辽宁海城某菱镁矿难选原因分析及浮选研究 [J]. *矿产综合利用*, 2021(2): 13–16.
- Wang E L, Li X A, Jiang X J, et al. Study on the analysis of refractory separation cause and flotation of Haicheng magnesite in Liaoning Province [J]. *Multipurpose Utilization of Mineral Resources*, 2021(2): 13–16.
- [21] 胡欢, 王汝成, 车旭东, 等. 关键金属元素铍的原位分析技术研究进展 [J]. *岩石学报*, 2022, 38(7): 1890–1900.
- Hu H, Wang R C, Che X D, et al. Research progress of *in situ* analysis technology of key metal element beryllium [J]. *Acta Petrologica Sinica*, 2022, 38(7): 1890–1900.
- [22] 范雨辰, 刘可禹, 蒲秀刚, 等. 页岩储集空间微观形态分类及三维结构重构——以渤海湾盆地沧东凹陷古近系孔店组二段为例 [J]. *石油勘探与开发*, 2022, 49(5): 943–954.
- Fan Y C, Liu K Y, Pu X G, et al. Morphological classification and three-dimensional pore structure reconstruction of shale oil reservoirs: A case from the second member of Kongdian Formation in the Cangdong Sag, Bohai Bay Basin, East China [J]. *Petroleum Exploration and Development*, 2022, 49(5): 943–954.
- [23] 王汉霞, 孟庆成, 张长捷. 隆昌地区辽河群岩石结构分析 [J]. *辽宁地质*, 1991(4): 305–313.
- Wang H X, Meng Q C, Zhang C J. Petrographic analysis of the Liaohe Formation in Longchang area [J]. *Liaoning Geology*, 1991(4): 305–313.
- [24] 郭进京. 辽东隆昌地区辽河群划分及其构造样式演变 [J]. *辽宁地质*, 1992(3): 255–263.
- Guo J J. Subdivision and tectonic style evolution of the Liaohe Formation in the Longchang area, Liaodong [J]. *Liaoning Geology*, 1992(3): 255–263.
- [25] 刘福来, 刘平华, 王舫, 等. 胶—辽—吉古元古代造山活动带巨量变沉积岩系的研究进展 [J]. *岩石学报*, 2015, 31(10): 2816–2846.
- Liu F L, Liu P H, Wang F, et al. Progresses and overviews of voluminous meta-sedimentary series within the Paleoproterozoic Jiao—Liao—Ji orogenic/mobile belt, North China Craton [J]. *Acta Petrologica Sinica*, 2015, 31(10): 2816–2846.
- [26] 杨中柱. 辽宁省区域地质志 [M]. 大连: 辽宁省地质勘查院, 2013, 28–44.
- Yang Z Z. Regional Geological Monograph of Liaoning Province [M]. Dalian: Liaoning Geological Exploration Institute, 2013, 28–44.
- [27] 肖仪武, 叶小璐, 武若晨, 等. 选矿产品矿物自动分析的光片制备 [J]. *中国无机分析化学*, 2020, 10(2): 1–6.
- Xiao Y W, Ye X L, Wu R C, et al. Polished section sample preparation of mineral processing products for mineral automatic analysis [J]. *Chinese Journal of Inorganic Analytical Chemistry*, 2020, 10(2): 1–6.
- [28] Figueroa G, Moeller K, Buhot M, et al. Advanced discrimination of hematite and magnetite by automated mineralogy [C]//Broekmans M. Proceedings of the 10th International Congress for Applied Mineralogy (ICAM). Heidelberg: Springer Press, 2014.
- [29] 徐登科. 矿物化学式计算方法 [M]. 北京: 地质出版社, 1977, 27–40.
- Xu D K. Methods for Calculating Mineral Chemical Formulas [M]. Beijing: Geological Publishing House, 1977, 27–40.
- [30] 池汝安, 王淀佐. 稀土选矿与提取技术 [M]. 北京: 科学出版社, 1996, 63–95.
- Chi R A, Wang D Z. Rare Earth Ore Beneficiation and Extraction Techniques [M]. Beijing: Science Press, 1996, 63–95.
- [31] Allanite H J. Thorium and light rare earth element carrier in subducted crust [J]. *Chemical Geology*, 2002, 192: 289–306.
- [32] 王汝成, 王硕, 邱检生, 等. 东海超高压榴辉岩中绿帘石、褐帘石、磷灰石和钛石集合体的电子探针成分和化学定年研究 [J]. *岩石学报*, 2006, 22(7): 1855–1866.
- Wang R C, Wang S, Qiu J S, et al. Electron-microprobe compositions and chemical dating of composite grains of epidote, allanite, apatite and Th-silicate from the Sulu UHP eclogites (CCSD main hole, Donghai, Eastern China) [J]. *Acta Petrologica Sinica*, 2006, 22(7): 1855–1866.
- [33] Shaw D M. Geochemistry of pelitic rocks [J]. *GSA*

- Bulletin, 1956, 67(7): 919–934.
- [34] 陈菲, 苏文, 张铭, 等. 褐帘石的谱学特征[J]. 岩石学报, 2019, 35(1): 233–242.
- Chen F, Su W, Zhang M, et al. Spectroscopic characteristics of the allanite[J]. *Acta Petrologica Sinica*, 2019, 35(1): 233–242.
- [35] Yakovenchuk V N, Krivovichev S V, Ivanyuk G Y, et al. Kihlmanite-(Ce), $\text{Ce}_2\text{TiO}_2[\text{SiO}_4](\text{HCO}_3)_2(\text{H}_2\text{O})$, a new rare-earth mineral from the pegmatites of the Khibiny alkaline massif, Kola Peninsula, Russia[J]. *Mineralogical Magazine*, 2014, 78(3): 483–496.
- [36] 周剑雄, 陈振宇, 芮宗瑶, 等. 独居石的电子探针钍-铀-铅化学测年[J]. 岩矿测试, 2002, 21(4): 241–246.
- Zhou J X, Chen Z Y, Rui Z Y. Th-U-Pb chemical dating of monazite by electron probe[J]. *Rock and Mineral Analysis*, 2002, 21(4): 241–246.
- [37] 梁晓, 徐亚军, 訾建威, 等. 独居石成因矿物学特征及其对U-Th-Pb年龄解释的制约[J]. 地球科学, 2022, 47(4): 1383–1398.
- Liang X, Xu Y J, Zi J W, et al. Genetic mineralogy of monazite and constraints on interpretation of U-Th-Pb ages[J]. *Earth Science*, 2022, 47(4): 1383–1398.
- [38] 王智琳, 许德如, Kusiak M A, 等. 海南石碌铁矿独居石的成因类型、化学定年及地质意义[J]. 岩石学报, 2015, 31(1): 200–216.
- Wang Z L, Xu D R, Kusiak M A, et al. Genesis of and CHIME dating on monazite in the Shilu iron ore deposit, Hainan Province of South China, and its geological implications[J]. *Acta Petrologica Sinica*, 2015, 31(1): 200–216.
- [39] Puchelt H, Emmermann R. Bearing of rare earth patterns of apatites from igneous and metamorphic rocks[J]. *Earth & Planetary Science Letters*, 1976, 31(2): 279–286.
- [40] 韦春婉, 许成, 付伟, 等. 稀土元素在岩浆和水热系统
- 的实验岩石学和地球化学研究进展[J]. *岩石学报*, 2022, 38(2): 455–471.
- Wei C W, Xu C, Fu W, et al. Research progress in experimental petrology and geochemistry of rare earth elements in magma and hydrothermal systems[J]. *Acta Petrologica Sinica*, 2022, 38(2): 455–471.
- [41] 朱笑青, 王中刚, 黄艳, 等. 磷灰石的稀土组成及其示踪意义[J]. 稀土, 2004, 25(5): 41–45, 63.
- Zhu X Q, Wang Z G, Huang Y, et al. Research advances in experimental petrology and geochemistry of rare earth elements in magmatic and hydrothermal systems[J]. *Acta Petrologica Sinica*, 2004, 25(5): 41–45, 63.
- [42] 饶金山, 刘超, 胡红喜, 等. 磷灰石含稀土机制与分离特性研究[J]. 稀土, 2021, 42(2): 84–93.
- Rao J S, Liu C, Hu H X, et al. Study on the mechanism and separation characteristics of rare earths in apatite[J]. *Rare Earths*, 2021, 42(2): 84–93.
- [43] Barker R D, Barker S L L, Wilson S A, et al. Quantitative mineral mapping of drill core surfaces I: A method for μ XRF mineral calculation and mapping of hydrothermally altered, fine-grained sedimentary rocks from a Carlin-type gold deposit[J]. *Economic Geology*, 2021, 116(4): 803–819.
- [44] Udayakumar S, Noor A F M, Rezan S A, et al. Chemical and mineralogical characterization of Malaysian monazite concentrate[J]. *Mining, Metallurgy & Exploration*, 2020, 37: 415–431.
- [45] Zhong J, Hu C, Fan H, et al. A new type U-Th-REE-Nb mineralization related to albite: A case study from the Chachaxiangka deposit in the Northeastern Qaidam Basin of China[J]. *China Geology*, 2019, 2(4): 422–438.
- [46] Redwan M, Rammler D, Nikonor W. Application of quantitative mineralogy on the neutralization-acid potential calculations within μm -scale stratified mine tailings[J]. *Environmental Earth Sciences*, 2017, 76(1): 46.